Quaternary Geochronology 53 (2019) 101007

Contents lists available at ScienceDirect

Quaternary Geochronology

journal homepage: www.elsevier.com/locate/quageo

Research paper

# Comparing the accuracy and precision of luminescence ages for partially-bleached sediments using single grains of K-feldspar and quartz

R.K. Smedley[a,*], J.-P. Buylaert[b,c], G. Újvári[b,d,e]

[a] Department of Geography and Planning, University of Liverpool, Liverpool, UK
[b] Center for Nuclear Technologies, Technical University of Denmark, DTU Risø Campus, Denmark
[c] Nordic Laboratory for Luminescence Dating, Department of Geoscience, Aarhus University, Risø Campus, DK-4000 Roskilde, Denmark
[d] Institute for Geological and Geochemical Research, Research Centre for Astronomy and Earth Sciences, Hungarian Academy of Sciences, H-1112 Budapest, Hungary
[e] Department of Lithospheric Research, University of Vienna, A-1090 Vienna, Austria

ARTICLE INFO

*Keywords:*
Single grains
Post-IR IRSL
K-feldspar
OSL
Quartz
Partially-bleached

ABSTRACT

Glacial settings are considered to be the most challenging context for the application of luminescence dating. The optically stimulated luminescence (OSL) signal of quartz is often preferred for luminescence dating in partially-bleached settings as it resets (or bleaches) more rapidly in response to sunlight than the post-IR IRSL (pIRIR) signal of K-feldspar, and can therefore better characterise the well-bleached part of the partially-bleached $D_e$ distribution. However, the relative bleaching extents of single grains of quartz and K-feldspar have not yet been compared for sedimentary samples from the natural environment. Here we compare the $D_e$ distributions and accuracy and precision of ages determined using single grains of quartz and K-feldspar from sedimentary samples deposited in a proglacial setting with independent age control. We found that the extent of bleaching of the OSL signal of quartz and $pIRIR_{225}$ signal of K-feldspar was similar (with similar over-dispersion), and therefore the $pIRIR_{225}$ signal bleached to similarly low levels as the OSL signal of quartz in this partially-bleached setting. We also observed a consistent offset in over-dispersion between quartz and K-feldspar of ~10% that can be linked to scatter arising from internal dose-rates of K-feldspar and should be included when applying age models. The results here demonstrate that the accuracy and precision of ages determined using the $pIRIR_{225}$ signal of single grains of K-feldspar were similar to the OSL signal of quartz. However, K-feldspars were 5–18 times more efficient than quartz at determining the population of interest for age calculation as a larger proportion of K-feldspar grains emitted a detectable luminescence signal in comparison to quartz. These findings contradict our current understanding of the bleaching of K-feldspar and quartz grains in the natural environment, and are likely applicable to other partially-bleached settings (e.g. fluvial, alluvial).

## 1. Introduction

Luminescence dating determines the time elapsed since a mineral grain (quartz or K-feldspar) was last exposed to sunlight and then buried in the natural environment. In environments where there are opportunities for prolonged exposure to sunlight (e.g. aeolian), the luminescence signals of individual grains are typically well bleached prior to burial (i.e. all grains were reset to zero). However, in settings where there are limited opportunities for sunlight exposure due to grains being transported and deposited by turbulent, sediment-laden water columns, the luminescence signals of grains are typically partially bleached prior to burial (i.e. only a proportion of the grains were reset to zero). By analysing single grains of quartz or K-feldspar, the well-bleached part of a partially-bleached $D_e$ distribution can be identified (Duller, 2008) and an accurate burial age can be determined using a minimum age model, e.g. the minimum age model (Galbraith and Laslett, 1993; Galbraith et al., 1999) or the internal external uncertainty (IEU) model (Thomsen et al., 2007).

Luminescence dating in partially-bleached settings often produces large age uncertainties (e.g. > 20%; Small et al., 2018) due to the difficulty in characterising the population of interest for age calculation in comparison to well-bleached sediments. In settings where there are limited opportunities for sunlight exposure, the optically stimulated luminescence (OSL) signal of quartz is often preferred for luminescence dating over the infra-red stimulated luminescence (IRSL) signals of K-feldspar as the OSL signal of quartz has the potential to bleach more rapidly in response to sunlight than the IRSL signals of K-feldspar (Godfrey-Smith et al., 1988; Buylaert et al., 2012; Colarossi et al.,

* Corresponding author.
*E-mail address:* rachel.smedley@liv.ac.uk (R.K. Smedley).

https://doi.org/10.1016/j.quageo.2019.101007
Received 29 January 2019; Received in revised form 18 June 2019; Accepted 18 June 2019
Available online 19 June 2019

2015). Therefore, it is more likely to be able to characterise the population of interest for age calculation better than the $pIRIR_{225}$ signal of K-feldspar. However, a major disadvantage of OSL dating of quartz in partially-bleached settings (e.g. glacial, fluvial) is that the OSL signals are usually dim (e.g. Preusser et al., 2006; Smedley et al., 2017a,b; Trauerstein et al., 2017) as the quartz grains have not experienced repeated, prolonged cycles of sunlight exposure and burial prior to burial, which is required to sensitise the OSL signal. Alternatively, the IRSL signals of K-feldspar can have an intrinsic brightness that is not dependent on sensitisation (e.g. Krbetschek et al., 1997). Therefore, in some settings it may be advantageous to use single grains of K-feldspar instead of quartz.

Studies have shown that single-grain $D_e$ distributions determined using the post-IR IRSL signal of K-feldspar could determine ages in agreement with the OSL signal of quartz for well-bleached sediments (e.g. Fu et al., 2015; Reimann et al., 2012). In contrast, only one glaciofluvial sample from alpine Switzerland has been used to compare the bleaching extents of both signals in a partially-bleached setting (Gaar et al., 2014), and many studies that do not use single-grain analyses suggest that the OSL signal of quartz is always better bleached than the post-IR IRSL signal of K-feldspar (e.g. Fu et al., 2015; Colarossi et al., 2015; Möller and Murray, 2015). At present, there is a lack of studies that directly compare the single-grain $D_e$ distributions and ages determined using the post-IR IRSL signal of K-feldspar and the OSL signal of quartz for partially-bleached sediments with independent age control. It is essential that we use single-grain analyses for this comparison as typically more K-feldspar grains give light than quartz grains; thus, any multiple-grain analyses would not be a fair comparison because the signal would be averaged across more grains for K-feldspar than quartz. Therefore, the aim of this study is to determine whether it would be more advantageous to use K-feldspar or quartz grains for luminescence dating in partially-bleached settings (e.g. glacial, fluvial, alluvial) by comparing the single-grain $D_e$ distributions, and accuracy and precision of ages. We use a suite of sediments deposited by the former British-Irish Ice Sheet that have experienced variable extents of bleaching prior to burial and have independent age control.

## 2. Methods

### 2.1. Sample descriptions

Seven sedimentary samples taken from proglacial sediments deposited during the retreat of the last British-Irish Ice Sheet were used in this study (Fig. 1). Each sample was constrained by independent age control provided by radiocarbon or cosmogenic nuclide dating (Table S1). The samples were taken from a range of depositional settings in a glacial environment and sourced from variable bedrock types. OSL analysis of quartz has shown that the samples had variable degrees of scatter in dose-recovery experiments arising from intrinsic luminescence characteristics (over-dispersion ranging from 0 to 30%; Table 1) and the extent of bleaching in nature due to variable scatter measured in the burial doses (over-dispersion ranging from 27 to 86%; Table 1). OSL ages for all the samples here have been previously published (see Table S1 for details).

### 2.2. Equivalent doses ($D_e$)

Grains of K-feldspar used to determine equivalent doses ($D_e$) were extracted by treating each sample with a 10% v/v dilution of 37% HCl and with 20% v/v of $H_2O_2$ to remove carbonates and organics, respectively. Dry sieving then isolated the 180–212 μm (sample T3COF4) or 212–250 μm (all other samples) diameter grains for all samples. Density separation using sodium polytungstate provided the 2.53–2.58 g $cm^{-3}$ (K-feldspar dominated) fractions, which were not etched using hydrofluoric acid. Finally, grains of K-feldspar were mounted on a 9.8 mm diameter aluminium single-grain disc for analysis, which contained a 10 by 10 grid of 300 μm diameter holes.

All luminescence measurements were performed using a Risø TL/OSL DA-15 automated single-grain system equipped with a $^{90}Sr/^{90}Y$ beta source (Bøtter-Jensen et al., 2003). The luminescence signal was detected through a blue filter pack (BG39, BG3) placed in front of the photomultiplier tube. Single aliquot regenerative dose (SAR) protocols (Murray and Wintle, 2000) were used for the post-IR IRSL analyses performed at both 225 °C (the $pIRIR_{225}$ signal) and 290 °C (the $pIRIR_{290}$ signal) (Thomsen et al., 2008; Thiel et al., 2011). The IRSL measurement performed at 50 °C within the $pIRIR_{225}$ protocol provided the $IR_{50/225}$ signal used for analysis. Preheat temperatures of 250 °C and 320 °C for 60 s were used prior to stimulations of 2 s using the infra-red laser at 50 °C and then 225 °C or 290 °C, respectively. An elevated temperature bleach of 330 °C for 200 s was performed using the IR LEDs at the end of each $L_x/T_x$ cycle. The location of the single-grain discs within the TL/OSL reader was checked at room temperature, rather than elevated temperatures to prevent thermal annealing of the IRSL signal (after Smedley and Duller, 2013). The first 0.3 s and final 0.6 s of stimulation were summed to calculate the initial and background IRSL signals, respectively.

The grains were accepted after applying the following screening criteria and accounting for the associated uncertainties: (1) whether the test dose response was greater than three sigma above the background, (2) whether the test dose uncertainty was less than 10%, (3) whether the recycling and OSL-IR depletion ratios were within the range of ratios 0.9 to 1.1, (4) whether recuperation was less than 5% of the response from the largest regenerative dose and (5) whether the single-grain $D_e$ values were not from a population of very low doses that were identified to be inconsistent with the geological context of the sample (i.e. < 1 ka) by the finite mixture model (FMM) using the $\sigma_b$ values estimated for each sample (Table 1). Note that only two K-feldspar grains (0.4% of the total number of grains analysed) from sample T4ADES01 failed this criteria. $D_e$ values were calculated from all grains passing all the screening criteria. The average dose model (ADM; Guérin et al., 2017) and the minimum age model (MAM; Galbraith and Laslett, 1993; Galbraith et al., 1999) were used to determine ages for samples deemed to have been well bleached and partially bleached prior to burial.

### 2.3. Dose-recovery experiments

Dose-recovery and residual dose experiments were performed using the $pIRIR_{225}$ signal on the K-feldspar grains from samples T3COF4, T4BATT03, T4ADES01, T4WEXF03 and T8SKIG02. The grains were first bleached for 16-h in a SOL2 solar simulator. The grains were then given a 16 Gy and a 0 Gy beta dose for the dose-recovery and residual dose experiments, respectively, before measuring the single-grain $D_e$ values using the protocols outlined in Section 2.2. The residual doses measured for each sample were then subtracted from the $D_e$ value determined for the dose-recovery experiments to assess the suitability of the SAR protocol. The results confirmed that the SAR protocol was appropriate as each sample could recover the given dose within ± 10%. The $D_e$ distributions determined for the dose-recovery experiments are shown in Fig. S1 and quantify the minimum over-dispersion arising from intrinsic sources of uncertainty shown in Table 1 (Thomsen et al., 2005); this ranged from 18 to 27% for the $pIRIR_{225}$ signal (Fig. S1). The over-dispersion values for the dose recovery dose distributions determined using quartz and K-feldspar did not correspond to one another, the over-dispersion values for samples T3COF4, T4BATT03 and T8SKIG02 were larger for the K-feldspar grains than quartz, while those for sample T4ADES01 were the same and the over-dispersion value for the K-feldspar grains for sample T4WEXF03 was lower than for quartz.

### 2.4. Dose-rates

External beta dose-rates were determined from U, Th, K and Rb

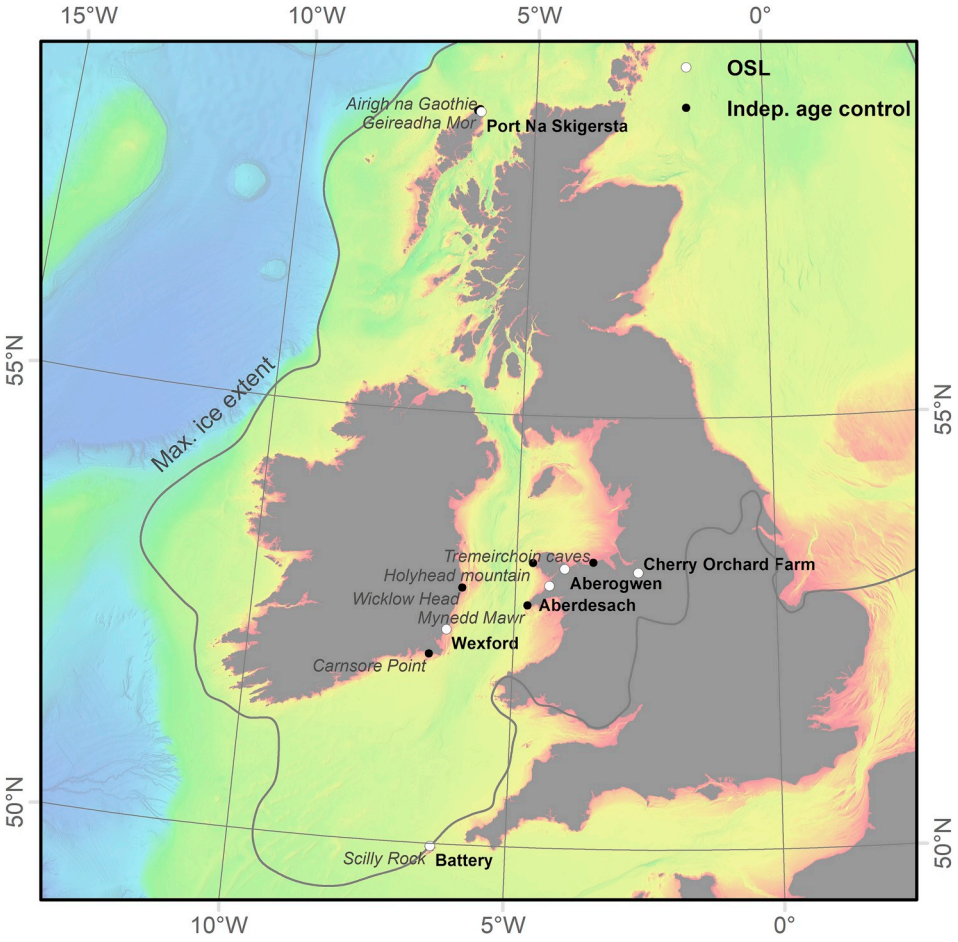


**Fig. 1.** Locations of the samples taken for luminescence dating in this study, in addition to the sites sampled for the existing independent age control, which is associated with the burial age of the luminescence samples. These are plotted over the European Marine Observation and Data Network (EMODnet, http://www.emodnet.eu) topographical data.

concentrations from milled and homogenised bulk sediment samples using inductively coupled plasma mass spectrometry (ICP-MS) and atomic emission spectroscopy (ICP-AES). External gamma dose-rates were determined using in-situ gamma spectrometry. Water contents were estimated considering the field and saturated water contents, and the environmental history for each sample. Cosmic dose-rates were calculated after Prescott and Hutton (1994). All dose-rate information is presented in Table S2.

Internal K-contents of density-separated fractions were determined for multiple-grain aliquots of each sample using an X-ray fluorescence spectrometer attachment on a Risø TL/OSL reader (Kook et al., 2012; Stevens et al., 2018). Internal K-contents were also measured for single

**Table 1**
Summary of luminescence dating using the OSL signal of quartz and the $pIRIR_{225}$ signal of K-feldspar for the same samples. The number of grains that were used to determine a $D_e$ value (n) are shown as a proportion of the total grains measured (N), in addition to the grain yield (n %). G-values (%/decade) were measured using the $pIRIR_{225}$ signal for three aliquots of K-feldspar for each sample, and are presented as weighted means and standard errors. Note that $\sigma_b$ was calculated for all samples and signals by combining the intrinsic overdispersion in quadrature with overdispersion arising from external microdosimetry (estimated at ~20% from $D_e$ distributions determined using the OSL signal of quartz as well bleached). All MAM $D_e$ values determined for K-feldspar included an additional 10% overdispersion added in quadrature due to the scatter caused by variability in the internal dose-rate. The uncertainty on the age is also presented as a percentage of the age (Uncertainty %). The independent age control was provided by Rowlands (1971)[1], Smedley et al. (2017a)[2], McCarroll et al. (2010)[3], Smedley et al. (2017b)[3], Small et al. (2018)[4] and Bradwell et al. (2019)[5] (see Table S1 for details).

| | | Dose-rate (Gy/ka) | Intrinsic OD (%) | G-value (%/dec.) | n/N | n (%) | Total OD (%) | Age Model | $\sigma_b$ | $D_e$ (Gy) | Age (ka) | Uncert. (%) | Independent age (ka) |
|---|---|---|---|---|---|---|---|---|---|---|---|---|---|
| T3COF4 | Kf | 1.93 ± 0.15 | 18 ± 1 | 1.3 ± 0.9 | 56/1200 | 5 | 71 ± 1 | MAM | 0.30 | 36.7 ± 5.0 | 19.0 ± 3.0 | 16 | ≤22.0 ± 3.6 cal ka |
| | Qtz | 1.13 ± 0.07 | 6 ± 1 | – | 73/7100 | 1 | 84 ± 1 | MAM | 0.20 | 31.1 ± 4.3 | 27.6 ± 4.2 | 15 | BP[1] |
| T4BATT03 | Kf | 2.99 ± 0.19 | 27 ± 1 | 1.4 ± 0.8 | 64/300 | 21 | 41 ± 1 | ADM | – | 82.0 ± 4.3 | 27.4 ± 2.2 | 8 | 25.9 ± 1.6[2] |
| | Qtz | 2.01 ± 0.10 | 5 ± 1 | – | 67/2600 | 3 | 38 ± 1 | ADM | – | 57.9 ± 3.2 | 28.8 ± 2.1 | 7 | |
| T4ADES01 | Kf | 3.19 ± 0.22 | 20 ± 1 | 1.3 ± 0.8 | 38/500 | 18 | 56 ± 1 | MAM | 0.30 | 57.0 ± 6.9 | 17.9 ± 2.5 | 14 | ≤25.1 ± 1.4[3] |
| | Qtz | 2.22 ± 0.13 | 21 ± 1 | – | 77/5900 | 1 | 48 ± 1 | MAM | 0.35 | 41.9 ± 6.5 | 18.9 ± 3.1 | 17 | ≥20.8 ± 1.2[3] |
| T4ABER01 | Kf | 3.34 ± 0.22 | – | 1.5 ± 0.7 | 63/300 | 21 | 46 ± 1 | ADM | – | 68.5 ± 3.9 | 20.5 ± 1.8 | 9 | ≤20.8 ± 1.2[3] |
| | Qtz | 2.35 ± 0.14 | 0 ± 0 | – | 33/2400 | 1 | 34 ± 1 | ADM | – | 45.1 ± 3.3 | 19.2 ± 1.8 | 9 | |
| T4WEXF03 | Kf | 1.49 ± 0.16 | 22 ± 1 | 2.1 ± 0.7 | 51/500 | 10 | 86 ± 1 | MAM | 0.30 | 29.1 ± 4.8 | 19.5 ± 3.8 | 19 | ≤25.8 ± 1.4[4] |
| | Qtz | 0.61 ± 0.03 | 30 ± 1 | – | 44/3700 | 1 | 86 ± 2 | MAM | 0.35 | 13.4 ± 2.8 | 21.8 ± 4.7 | 22 | ≥21.2 ± 1.9[4] |
| T8SKIG01 | Kf | 2.56 ± 0.20 | - | 1.1 ± 0.7 | 124/300 | 41 | 38 ± 1 | MAM | 0.35 | 61.6 ± 6.1 | 24.1 ± 3.1 | 13 | ≤26.4 ± 1.5[5] |
| | Qtz | 1.64 ± 0.10 | - | – | 70/900 | 8 | 39 ± 1 | MAM | 0.25 | 37.8 ± 2.4 | 23.1 ± 2.1 | 9 | ≥21.6 ± 1.2[5] |
| T8SKIG02 | Kf | 2.40 ± 0.20 | 25 ± 1 | 0.8 ± 0.6 | 128/300 | 43 | 45 ± 1 | ADM | – | 58.0 ± 2.6 | 24.2 ± 2.3 | 9 | ≤26.4 ± 1.5[5] |
| | Qtz | 1.48 ± 0.10 | 15 ± 1 | – | 81/1000 | 8 | 27 ± 0 | ADM | – | 33.9 ± 1.2 | 23.0 ± 1.8 | 8 | ≥21.6 ± 1.2[5] |

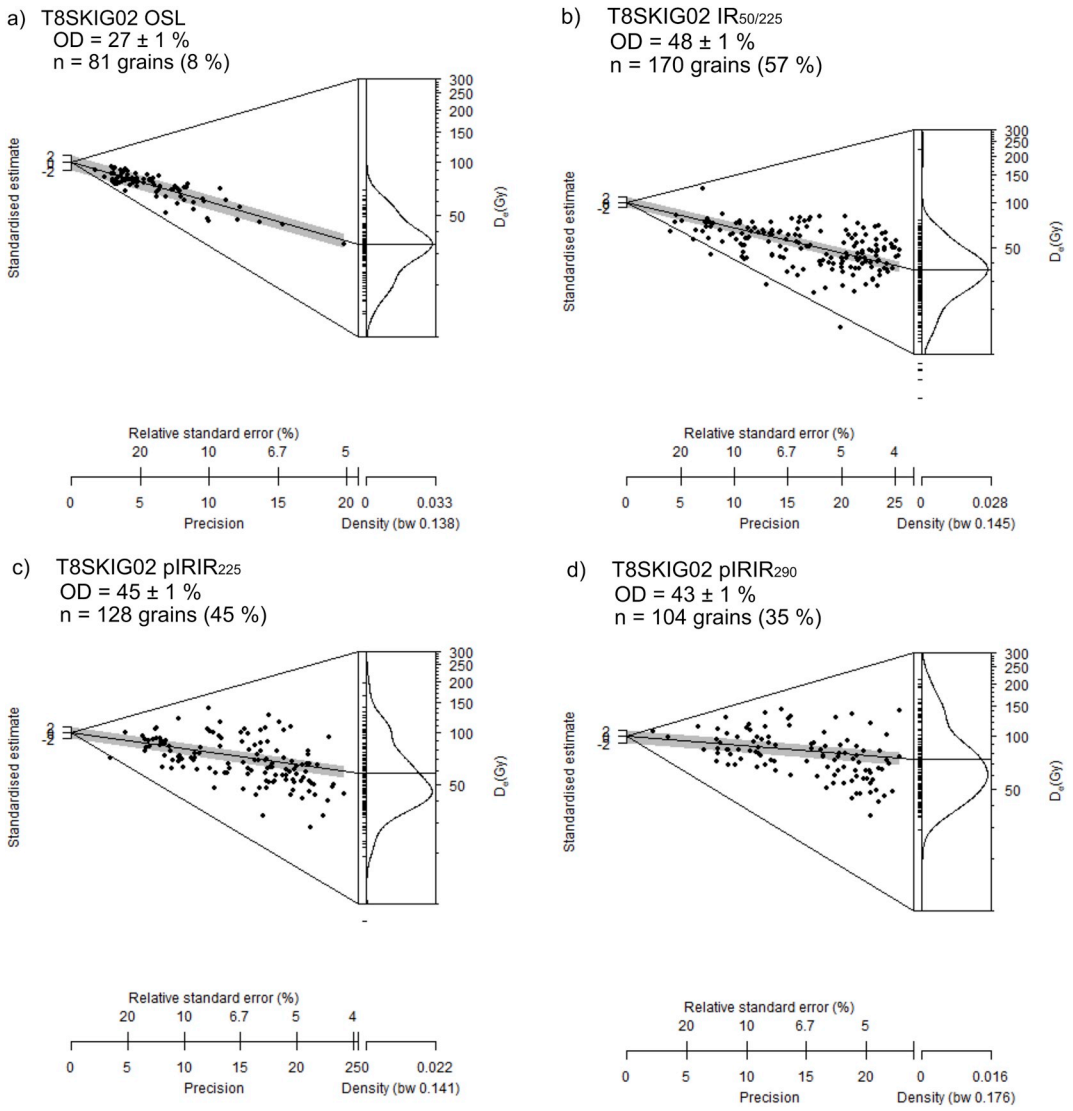


**Fig. 2.** Abanico plots of the single-grain $D_e$ distributions for sample T8SKIG02 determined using the OSL signal of quartz and $IR_{50/225}$, $pIRIR_{225}$ and $pIRIR_{290}$ signals of K-feldspar. The grey bar highlights the ADM $D_e$ value determined for the $D_e$ distribution ( ± 1 σ).

grains of sample T8SKIG02 that had previously been measured for a $D_e$ value. Grains were kept in the single-grain disc and placed directly into a Brüker M4 Tornado μ-XRF instrument (beam spot size: ~25 μm, effective K, Ca sampling depth ~30 μm, Na ~5 μm) after Buylaert et al. (2019). Internal K-contents were calculated as a mean ( ± standard error) of three repeated measurements on the same grain (acquisition time 45 s each).

## 3. Signal selection

The use of different signals for luminescence dating of K-feldspar was assessed using sample T8SKIG02 as the single-grain $D_e$ distribution determined using the OSL signal of quartz had the lowest $D_e$ value of all the samples (Fig. 2a; over-dispersion = 27 ± 1%). The single-grain $D_e$ distributions determined using the $IR_{50/225}$ signal of K-feldspar (Fig. 2b) extended to lower $D_e$ values than the equivalent $D_e$ distributions determined using the $pIRIR_{225}$ signal of K-feldspar (Fig. 2c). It is likely that this reflects the larger fading rates of the $IR_{50/225}$ signal from single grains in comparison to the $pIRIR_{225}$ signal, or that such signals are prone to sensitivity changes that are not correctly monitored by the SAR protocol (Kars et al., 2014a). The $IR_{50/225}$ age (14.9 ± 1.4 ka) for sample T8SKIG02 (Fig. 3) underestimated the OSL age determined from

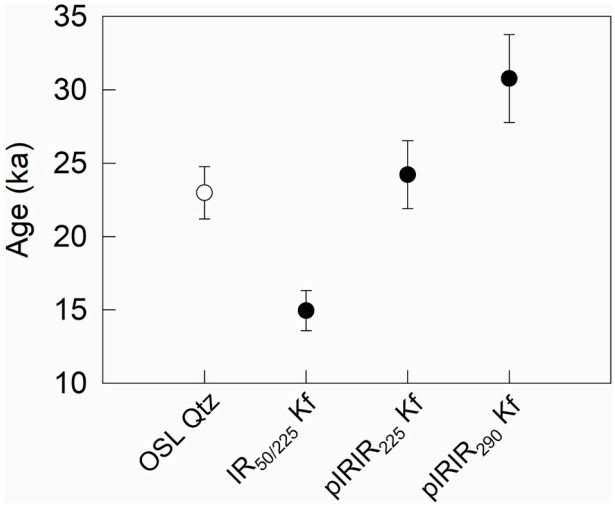


**Fig. 3.** Comparison of ages for sample T8SKIG02 determined using the OSL signal of quartz and $IR_{50/225}$, $pIRIR_{225}$ and $pIRIR_{290}$ signals of K-feldspar.

quartz (23.0 ± 1.8 ka), which also suggests the $IR_{50/225}$ signal is suffering from anomalous fading and requires fading correction. However, performing accurate single grain fading measurements and corrections is difficult and so a post-IR IRSL signal is preferred for further analysis here.

The single-grain $D_e$ values determined from K-feldspar for sample T8SKIG02 extended to larger doses using the $pIRIR_{290}$ signal (Fig. 2d) than the $pIRIR_{225}$ signal (Fig. 2c). Also, the $pIRIR_{290}$ signal yielded an older age for sample T8SKIG02 (30.8 ± 3.0 ka) than the $pIRIR_{225}$ signal (24.2 ± 2.3 ka) and the OSL signal of quartz (23.0 ± 1.8 ka) (Fig. 3). This may suggest poor dose recovery of the $pIRIR_{290}$ signal (e.g. Qin et al., 2018 and references therein) or reflect that the $pIRIR_{290}$ signal is more difficult to bleach in nature than the $pIRIR_{225}$ signal and the OSL signal of quartz. The latter is consistent with Smedley et al. (2015) who demonstrated that the $pIRIR_{225}$ signal of most K-feldspar grains can bleach to similarly low levels, whereas the bleaching rates for the $pIRIR_{290}$ signal of individual K-feldspar grains was more variable between grains, with fewer grains bleaching to lower levels than the $pIRIR_{225}$ signal. Given that the inherent bleaching rate of the pIRIR signal is likely important when grains are deposited in environments with limited opportunities for sunlight exposure prior to burial, the $pIRIR_{290}$ signal of K-feldspar was not used for analyses here. Alternatively, the $pIRIR_{225}$ signal was used to determine luminescence ages for K-feldspar for the suite of proglacial sediments and compared to results determined using the OSL signal of quartz; this is consistent with previous studies performed in glacial settings (e.g. Smedley et al., 2016).

## 4. Total dose-rates

The total dose-rates calculated for the density-separated K-feldspar fraction of the seven samples ranged from 1.49 ± 0.16 to 3.34 ± 0.22 Gy/ka (Table S2). The purity of the density-separated fraction was assessed on a multiple-grain basis using XRF (Fig. 4a). The results suggest that the 2.53–2.58 g $cm^{-3}$ (K-feldspar dominated) fractions were ~10–14% K, while the 2.58–2.62 g $cm^{-3}$ (Na-feldspar dominated) fractions were ~4–8% K. The K-content of the < 2.53 g $cm^{-3}$ fraction was also measured to assess the effectiveness of this density separation for these samples. The results suggest that the < 2.53 g $cm^{-3}$ fraction had similar K-contents to the K-feldspar-dominated fraction (2.53–2.58 g $cm^{-3}$), and therefore that separating at 2.53 g $cm^{-3}$ made little difference to the bulk K-content of the density-separated K-feldspar fraction. However, it is possible that density separation at 2.53 g $cm^{-3}$ may have removed a small proportion of individual grains with weathering coatings and/or products which were undetectable to the multiple-grain XRF measurements.

The internal K-contents of single grains of the K-feldspar separate were assessed for a subsample of 59 randomly selected grains from sample T8SKIG02 using a μXRF. The results suggested that the K-feldspar separate was composed of variable feldspar types, including both alkali and plagioclase feldspars (Fig. 4b), with internal K-contents ranging from 0 to 14%. The mean ± standard error of the single grain measurements was 8 ± 1% K, which is broadly consistent with the multiple-grain measurement (10% K), given that the μXRF was performed on a different subset of 59 grains. The internal K-contents are compared to the $T_n$ signal-intensity emitted by each grain for the $pIRIR_{225}$ signal (Fig. 5a) and suggest that the brightest grains are those of end member composition, but that measurable $pIRIR_{225}$ signals can be emitted from grains with internal K-content ranging from 0 to 14% K, where the proportion of grains equated to 14% (0–2% K), 5% (2–4% K), 0% (4–6% K), 5% (6–8% K), 24% (8–10% K), 10% (10–12% K) and 43% (12–14% K). Only for 21 out of the 59 randomly selected grains a $D_e$ value was determined using the $pIRIR_{225}$ signal (Fig. 5b). These grains tended towards the end member compositions, where 81% of the grains giving $D_e$ values had internal K-contents > 7% and 19% had internal K-contents < 3%. If the internal beta dose-rate provided by K within the feldspar grain was a dominant control of the single-grain $D_e$ distribution, then there would be a relationship between the internal K-content and the single-grain $D_e$ values. However, Fig. 5b shows that there was no relationship between internal K-content and $D_e$ value, which is consistent to findings from previous studies (e.g. Buylaert et al., 2019; Smedley et al., 2016; Trauerstein et al., 2014). Therefore it is likely that any relationship between $D_e$ and the internal K-content is masked by scatter arising from a combination of additional factors such as the extent of bleaching in nature, intrinsic luminescence characteristics and/or external microdosimetry. Moreover, Buylaert et al. (2019) suggest that there is significant variability in single-grain internal Rb concentrations that do not correspond to internal K-contents and also that single grain measurements of K-feldspar are not as accurate as we often assume; these factors may also mask any such relationship.

The mean ± standard error internal K-content of the 21 grains analysed using the μXRF (9 ± 1% K) is similar to that determined from multiple grains of sample T8SKIG02 using multi-grain XRF (10% K); this is consistent with the suggestion of Smedley et al. (2012) that an internal K-content of 10 ± 2% should be applied to account for the variability observed in grains used to determine $D_e$ values from a density-separated K-feldspar fraction. Applying an assumed internal K-content of 10 ± 2% included 38% of the grains within ± 2% K

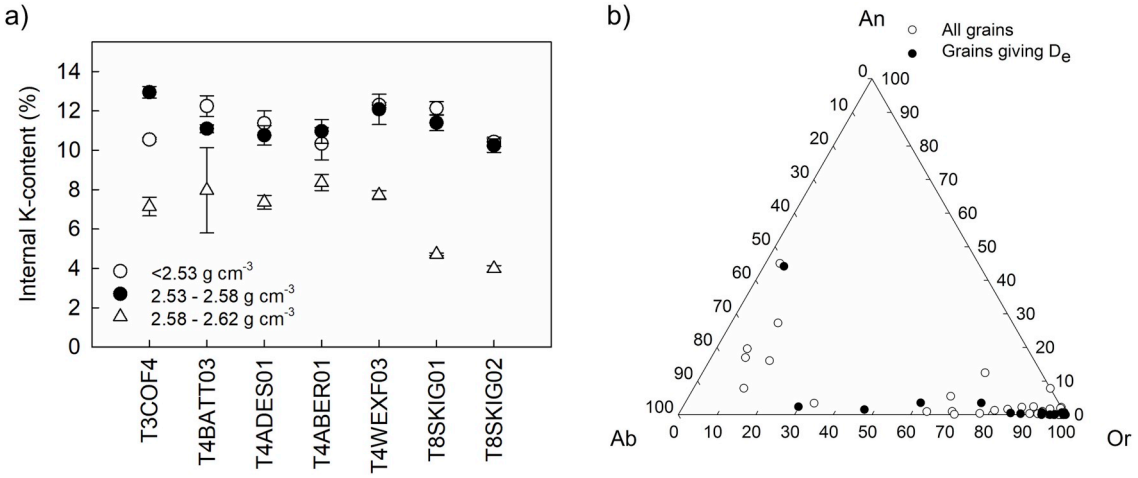


**Fig. 4.** (a) Internal K-contents (mean ± standard deviation of three measurements) for multiple grains of the density-separated feldspar fractions determined using the XRF. (b) Ternary diagram showing the feldspar compositions of individual grains analysed using the μXRF. Note that all values shown are the mean of three measurements and range from orthoclase (Or; K-rich), to albite (Ab; Na-rich) to anorthoclase (An; Ca-rich).

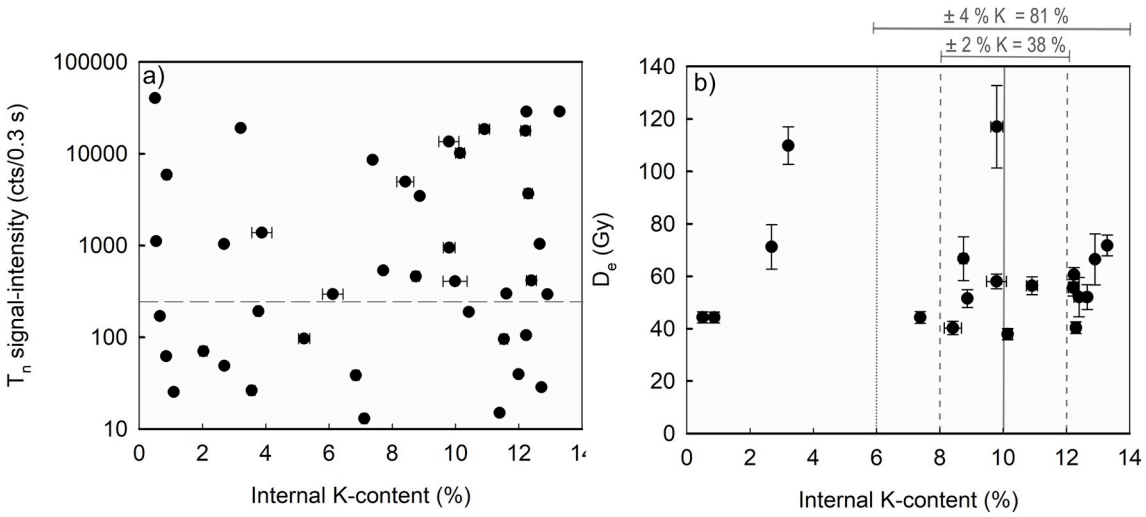


**Fig. 5.** Internal K-content (mean ± standard error of three measurements) determined from the μXRF plotted against the response to a test-dose ($T_n$) (a) and $D_e$ values (b) for the $pIRIR_{225}$ signals of K-feldspar grains. The dashed grey line in (a) marks the approximate signal-intensity screening criteria threshold. The solid grey line in (b) marks an internal K-content of 10%, while the dashed and dotted grey lines mark ± 2% and ± 4% K, respectively.

(i.e. ± 1 σ) and 81% of the grains within ± 4% K (i.e. ± 2 σ). Smedley and Pearce (2016) used LA-ICP-MS to measure mean ( ± standard error) internal U and Th concentrations of 0.3 ± 0.1 ppm and 1.7 ± 0.4 ppm, respectively, for a sample that contained similarly variable internal K-contents to those analysed here (Fig. 5a and b). Therefore, internal U and Th concentrations of 0.3 ± 0.1 ppm and 1.7 ± 0.4 ppm, respectively were applied to determine the corresponding internal alpha and beta dose-rates.

## 5. Anomalous fading

Fading experiments were performed on three multiple-grain aliquots (2 mm in diameter) per sample after each sample had been stimulated for 500 s at 290 °C (90% power) using the IR LEDs to remove any natural dose. Each aliquot was given a 21 Gy dose and $L_x/T_x$ values were determined using the SAR protocol, but where different delay times were inserted in between the preheat and IR stimulation; this included a prompt measurement and delay times of ca. 1 h, 5 h and 10 h. The prompt measurement was recycled and all aliquots determined $L_x/T_x$ values that were within ± 1 σ of one another. Fading rates (*g*-values, Aitken, 1985) were then determined for each aliquot and normalised to a $t_c$ of two days (Huntley and Lamothe, 2001, Fig. 6). The uncertainties on the individual *g*-values measured varied from 1.1 to 1.6% due to the large uncertainty in the fit of the data, which is typical of fading measurements for the pIRIR signal (e.g. Smedley et al., 2016). To derive a more reliable estimate of the fading rate, the weighted mean and standard error was calculated for $pIRIR_{225}$ signals (1.4 ± 0.3%/decade), and was lower than the corresponding *g*-value for the $IR_{50/225}$ signal (2.9 ± 0.2%/decade). Given that the $pIRIR_{225}$ fading rate is low (≤1.5%/decade) for each sample (Table 1) and in line with earlier $pIRIR_{225}$ studies (e.g. Roberts, 2012; Trauerstein et al., 2014; Kolb and Fuchs, 2018), we did not correct the $pIRIR_{225}$ ages for fading.

## 6. Signal-intensity distribution

The $pIRIR_{225}$ signal emitted from K-feldspar grains was generally brighter than the OSL signal emitted from quartz grains for the same

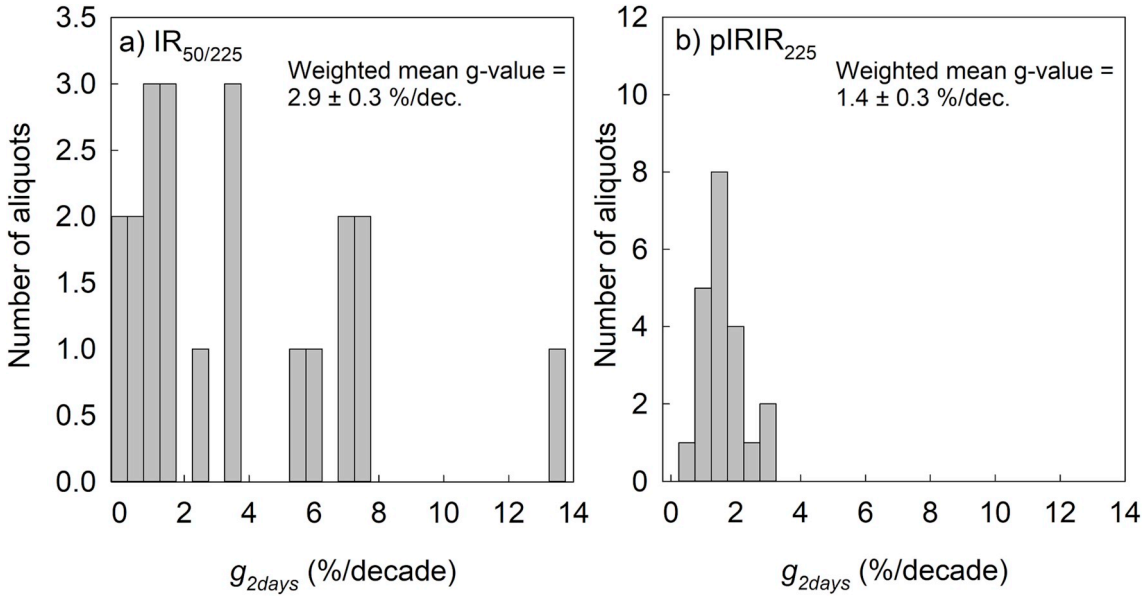


**Fig. 6.** Histograms of the individual *g*-values determined for aliquots of samples in this study (three per sample).

sample. The cumulative light sum plots which are based on the test-dose signal recorded after the natural luminescence measurement (Fig. S2) show that a larger proportion of K-feldspar grains emitted a measurable signal in comparison to the number of grains emitting a measurable OSL signal from quartz. A total of 90% of the OSL signal emitted by quartz grains was from 4 to 16% of the brightest grains, whereas 90% of the $pIRIR_{225}$ signal emitted by K-feldspar grains was from 14 to 45% of the brightest grains. The greatest difference was observed for sample T3COF4 where 90% of the brightest $pIRIR_{225}$ signal was emitted by 45% of the K-feldspar grains, while 90% of the brightest OSL signal was emitted by 13% of the quartz grains (Fig. S2a). This difference in signal intensities emitted by individual grains of quartz and K-feldspar translated into a greater number of K-feldspar grains passing the screening criterion and determining a $D_e$ value than quartz (Table 1; Fig. S2). The $D_e$ yield for the K-feldspar grains from all the samples ranged from 6 to 57% of all the grains analysed, which was significantly larger in comparison to the range of quartz grains from 1 to 8% (Table 1).

## 7. Burial ages

The single-grain $D_e$ distributions determined using the $pIRIR_{225}$ signal of K-feldspar and the OSL signal of quartz for each sample are shown together in Fig. 7. To determine accurate ages for partially-bleached samples, it is important to quantify the amount of scatter that would be inherent to the $D_e$ distribution if it had been well bleached prior to burial so that those grains that form the well bleached part of the partially-bleached $D_e$ distribution can be identified; this is referred to as $\sigma_b$ for the MAM. The scatter in a single-grain $D_e$ distribution determined using the $pIRIR_{225}$ signal of K-feldspar that was well bleached prior to burial will arise from grain-to-grain variations in internal dose-rate and anomalous fading, in addition to the factors that are also characteristic of quartz (intrinsic luminescence characteristics, external microdosimetry). The over-dispersion arising from variability in intrinsic luminescence characteristics (Thomsen et al., 2005) was quantified using beta dose-recovery experiments (Table 1; Fig. S1), while over-dispersion of ~20% was assumed to have arisen from external microdosimetry similar to that observed for quartz (Smedley et al., 2017b). Note that the relative over-dispersion arising from external microdosimetry will be slightly lower for K-feldspar than quartz as a proportion of the total dose-rate for K-feldspar is provided by an internal dose-rate whereas quartz is internally inert. However, most of the samples in this study have relatively high dose rates where the internal beta dose-rate contributes only ~20–30% of total dose rate, and so the discrepancy in the over-dispersion caused by external microdosimetry for quartz and K-feldspar is likely to be small. For sample T4WEXF03, the internal beta dose-rate contributes 46% of the total dose-rate and so the difference in over-dispersion for quartz and K-feldspar caused by external microdosimetry is likely to be larger; however, the contribution of partial bleaching to the over-dispersion is dominating the $D_e$ distribution in comparison to other factors.

The amount of over-dispersion expected to have been caused by internal dose-rates in the single-grain $D_e$ distributions was estimated using grain-specific dose-rates calculated from the μXRF results. The absolute standard deviation of the grain-specific dose-rates was divided by the total dose rate to estimate an over-dispersion value for the $D_e$ distribution that was arising solely from variability between grains in the internal beta dose-rates. The over-dispersion estimated to have arisen from the internal dose-rates for only those grains from the K-feldspar separate that gave $D_e$ values using the $pIRIR_{225}$ signal was 13%. This estimates that an additional ~10% should be added in quadrature when determining the $\sigma_b$ value for MAM to account for the scatter arising from internal dose-rates, which is consistent with the ~10% (GDNZ13) suggested by Smedley and Pearce (2016) for an aeolian sand from New Zealand with similar geochemical composition. Given that the $pIRIR_{225}$ signal was used to determine the single-grain $D_e$ distributions and the fading was negligible (Section 5), no additional scatter was incorporated into $\sigma_b$ to account for variability caused by anomalous fading. The scatter arising from variability in intrinsic luminescence characteristics, external microdosimetry and internal dose-rates were combined in quadrature to determine $\sigma_b$ for the MAM. The $pIRIR_{225}$ ages calculated for all the samples are plotted against the quartz OSL ages in Fig. 8a and the over-dispersion is shown in Fig. 8b.

## 8. Discussion

The single-grain $D_e$ distributions determined for quartz and K-feldspar for the same samples were broadly consistent as evidenced by a relationship between quartz and K-feldspar over-dispersion values (Fig. 8b). When the over-dispersion data were fit with a linear function, the size of the intercept (~13%) on the K-feldspar axis can potentially be explained by the over-dispersion arising from internal dose-rate variations estimated at 13% from μXRF measurements. For six out of the seven samples (samples T4BATT03, T4ADES01, T4ABER01, T4WEXF03, T8SKIG01 and T8SKIG02), there was good agreement between the ages determined using the $pIRIR_{225}$ signal of K-feldspars and the OSL signal of quartz, in addition to the independent age control (Table 1). However, for sample T3COF4, the age determined using the $pIRIR_{225}$ signal was younger than the OSL signal of quartz (Fig. 8a), but agreed with the independent age control (Table S1). Some independent age control for sample T3COF4 is provided by a radiocarbon age of a mammoth bone in the Tremeirchoin cave, NE Wales, which is overlain by till. When the radiocarbon age was re-calibrated using INTCAL13, it suggests that the till was deposited $\leq 22.0 \pm 3.6$ cal ka BP (Table S1), but there is some uncertainty over the reliability of this radiocarbon age. The accuracy of this radiocarbon age is supported by the Bayesian Sequence model for ice retreat across the northern Irish Sea Basin incorporating cosmogenic nuclide and luminescence ages determined using single grains of quartz, which constrains retreat to the Isle of Man after ice has pulled-back from the Cheshire Plains to $20.8 \pm 0.7$ ka (Chiverrell et al., 2018). However, the large uncertainty on the quartz OSL age means that no firm conclusion can be drawn from the comparison with independent age control.

The $D_e$ distributions of sample T3COF4 determined using both quartz (Fig. 7b) and K-feldspar (Fig. 7a) were broadly bimodal. Both $D_e$ distributions suggest that very few grains in this sample were well bleached prior to burial and that this sample has therefore experienced very limited exposure to sunlight. This very poor bleaching was likely because the grains were transported in a deeper water column than the other sedimentary samples in this study; this has been interpreted from the sedimentary characteristics. Given that the $pIRIR_{225}$ signal of K-feldspar grains reset more slowly in response to sunlight than the OSL signal of quartz (Colarossi et al., 2015), it is expected that the resulting single-grain $D_e$ distributions determined from K-feldspar would not be reset to similar extents to those determined from quartz in such deep water settings; however, the single-grain $D_e$ distributions measured for T3COF4 using K-feldspar and quartz were similar. Previous studies have shown how shorter wavelengths that are more efficient at bleaching the OSL signal of quartz are attenuated to greater extents in turbid water columns in comparison to the wavelengths that are more efficient at bleaching the IRSL signals of K-feldspar (e.g. Jerlov, 1970; Kronborg, 1983; Sanderson et al., 2007). This may explain how the luminescence signals of K-feldspar grains were reset to similar extents in the deep water column as the quartz grains.

The agreement between the $D_e$ distributions (Fig. 7; Fig. 8b) and ages (Fig. 8a) determined using the $pIRIR_{225}$ signal of K-feldspar and OSL signal of quartz suggests that the extent of bleaching in nature (or external microdosimetry) was likely the most dominant sources of scatter in these samples. More importantly, the consistency between the $D_e$ distributions suggests that the $pIRIR_{225}$ signals emitted by single grains of K-feldspar were bleached to similar extents as the OSL signals of single grains of quartz in this proglacial setting. This is consistent

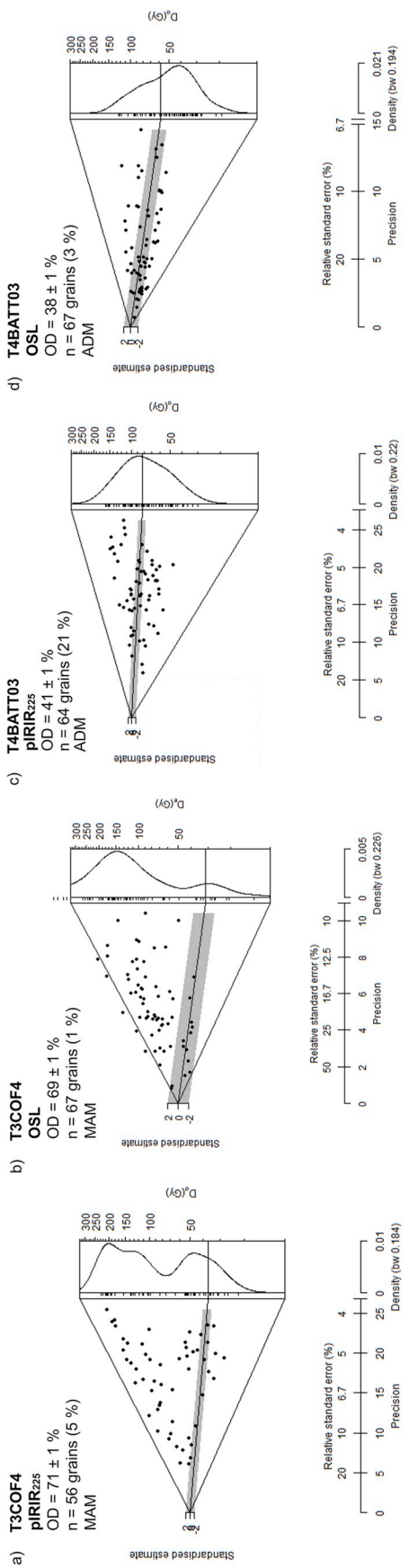


**Fig. 7.** Abanico plots of the single-grain $D_e$ distributions determined using the OSL signal of quartz and the $pIRIR_{225}$ of K-feldspar. The grey shading marks the ADM or MAM $D_e$ value calculated for each $D_e$ distribution. The $D_e$ distributions determined using the OSL signal of quartz were previously published for samples T3COF4 (Chiverrell et al. in prep), T4BATT03 (Smedley et al., 2017a), T4ADES01. T4ABER01 (Smedley et al., 2017b), T4WEXF03 (Small et al., 2018), T8SKIG01 and T8SKIG02 (Bradwell et al., 2019).

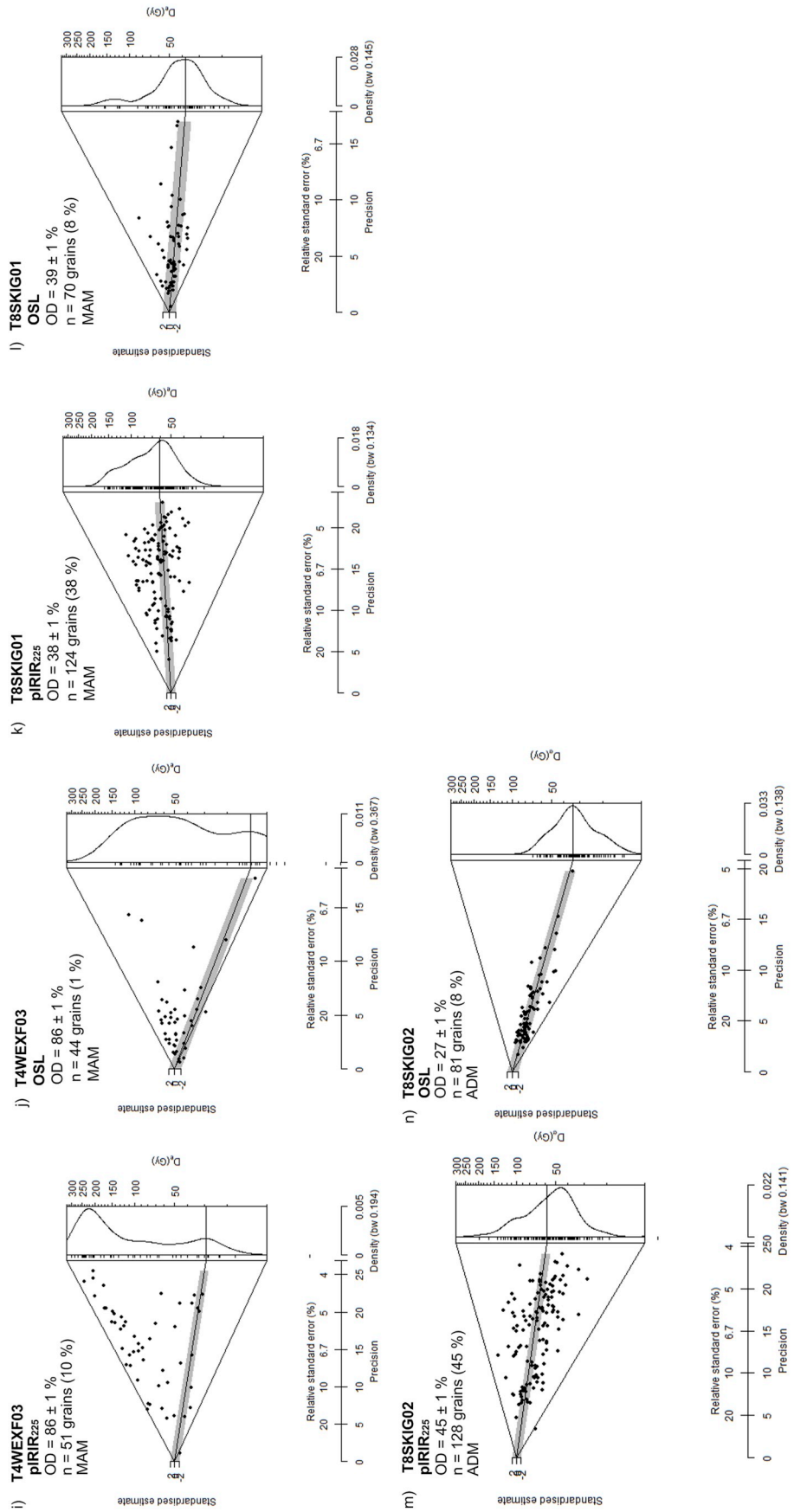


**Fig. 7.** (*continued*)

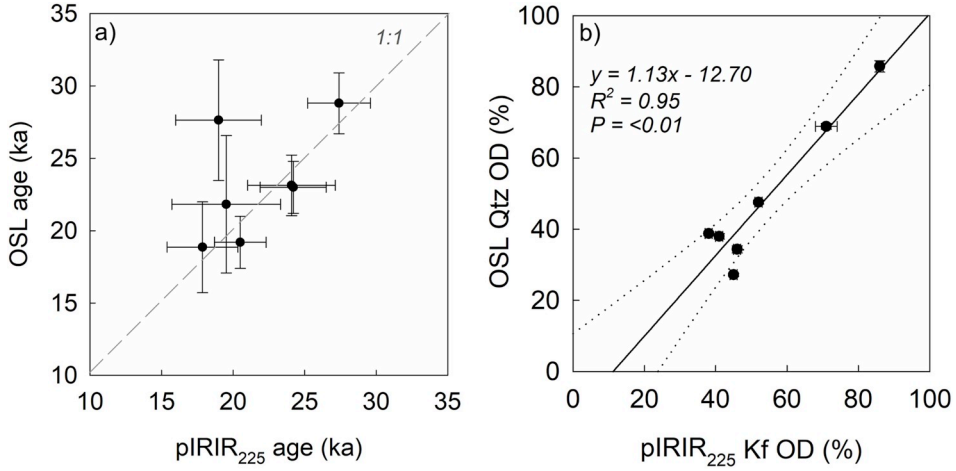


**Fig. 8.** Comparison of the luminescence ages (a), and overdispersion (OD) (b) determined from single-grain $D_e$ values determined for each sample using the OSL signal of quartz and $pIRIR_{225}$ signal of K-feldspar. Note that the errors bars show ± 1 σ ranges for each datapoint.

with the findings of King et al. (2014) which suggest that the quartz OSL signal, $IRSL_{50}$ and post-IR $IRSL_{250}$ signals of K-feldspar bleached at the same rate across the same bar feature on a proglacial outwash plain of a modern glacier in Norway. Our data suggest that any residual doses incorporated into the burial dose caused by the slower bleaching rate of the $pIRIR_{225}$ signal in comparison to the OSL signal of quartz were negligible in comparison to the burial dose, or the small residual dose is compensated by small fading rates (e.g. Kars et al., 2014b). This provides data from the natural environment to support the laboratory experiments of Smedley et al. (2015) which showed that the $pIRIR_{225}$ signal of most grains bleach similarly to low levels in response to sunlight. Therefore, the $pIRIR_{225}$ signal of single grains of K-feldspar can characterise the last depositional cycle that grains have experienced prior to burial. By fully characterising the well-bleached part of a partially-bleached $D_e$ distribution, the $pIRIR_{225}$ signal of single grains of K-feldspar can determine accurate luminescence ages in partially-bleached environments where grains have limited exposure to sunlight (e.g. glacial, fluvial, alluvial). Moreover, the precision of the OSL ages determined using the $pIRIR_{225}$ signal of K-feldspars is similar to the OSL signal of quartz (Table 1) as a similar proportion of grains can characterise the minimum age population. However, due to the larger proportion of K-feldspar grains emitting a measurable signal in comparison to the OSL signal of quartz, luminescence dating of K-feldspar was 5–18 times more efficient than quartz at determining $D_e$ values in the population of interest used for age calculation.

The more even distribution of signal-intensity across K-feldspar grains shows that characterising the true nature of a partially-bleached $D_e$ distribution would be more difficult when the signal is averaged across multiple-grain aliquots in comparison to quartz. Greater signal averaging across K-feldspar grains in comparison to quartz may explain the discrepancy between OSL ages for quartz and K-feldspar published in other studies which is alternatively linked to residual doses of K-feldspar (e.g. Fu et al., 2015; Colarossi et al., 2015; Möller and Murray, 2015). By comparing $D_e$ distributions from single grains of quartz and K-feldspar, we provide a reliable test of relative bleaching in nature and demonstrate that K-feldspar can be used to provide accurate and precise ages in partially-bleached environments when the signal analysed is from a single grain.

## 9. Conclusion

Glacial settings are considered to be the most challenging context for the application of luminescence dating and often produce large age uncertainties due to the difficulty in characterising the population of interest for age calculation in comparison to well-bleached settings. The OSL signal of quartz is often preferred over the post-IR IRSL signal of K-feldspar for luminescence dating in glacial settings as the OSL signal has greater potential to bleach rapidly in response to sunlight exposure. Therefore, the OSL signal of quartz may better characterise the well-bleached part of the partially-bleached $D_e$ distribution than K-feldspar. However, this has never been tested using $D_e$ distributions determined using single grains of both quartz and K-feldspar for a suite of partially-bleached samples with independent age control. Here we present single-grain $D_e$ distributions for partially-bleached sediments which suggest that the extent of bleaching of the OSL signal of quartz and $pIRIR_{225}$ signal of K-feldspar was similar (with similar over-dispersion). Therefore, the $pIRIR_{225}$ signal has the potential to bleach to similarly low levels as the OSL signal of quartz in partially-bleached environments. When comparing the over-dispersion values determined for the OSL signal of quartz and $pIRIR_{225}$ signal of K-feldspar, there was a systematic offset of ~10% over-dispersion, which could be explained by scatter caused by variability in the internal dose-rates of K-feldspar; thus, an additional 10% was incorporated when applying age models. The new findings here demonstrate that the $pIRIR_{225}$ signal of K-feldspar can be used to determine luminescence ages in glacial settings and produce ages with similar accuracy and precision as the OSL signal of quartz. However, due to the larger proportion of K-feldspar grains emitting a measurable signal in comparison to the OSL signal of quartz, luminescence dating of K-feldspar was 5–18 times more efficient than quartz at determining $D_e$ values in the population of interest used for age calculation. These findings are in contrast to our existing understanding of the bleaching of K-feldspar and quartz grains in the natural environment, and are also likelyapplicable to other partially-bleached settings (e.g. fluvial, alluvial).

## Acknowledgements

The samples in this study were originally used to determine OSL ages for quartz as part of the BRITICE-CHRONO project, a Natural Environment Research Council consortium grant (NE/J008672/1). Thanks to D. Small for providing the information on the independent age control. J.-P. Buylaert and G. Újvári received funding from the European Research Council under the European Union Horizon 2020 research and innovation programme ERC-2014-StG 639904 – RELOS. R. Smedley benefited from a AUFF guest researcher grant (AUFF-F-2018-6-1 1) awarded by Aarhus University.

## Appendix A. Supplementary data

Supplementary data to this article can be found online at https://doi.org/10.1016/j.quageo.2019.101007.

## References


Aitken, M.J., 1985. Thermoluminescence Dating. Academic, New York, pp. 359.

Bøtter-Jensen, L., Andersen, C.E., Duller, G.A.T., Murray, A.S., 2003. Developments in radiation, stimulation and observation facilities in luminescence measurements. Radiat. Meas. 37, 535–541.

Buylaert, J.-P., Újvári, G., Murray, A.S., Smedley, R.K., Kook, M., 2019. On the relationship between K concentration, grain size and dose in feldspar. Radiat. Meas. 120, 181–187.

Buylaert, J.-P., Jain, M., Murray, A.S., Thomsen, K.J., Thiel, C., Sobhati, R., 2012. A robust feldspar luminescence dating method for Middle and Late Pleistocene sediments. Boreas 41 (3), 435–451.

Bradwell, T., Small, D., Fabel, D., Smedley, R.K., Clark, C., Saher, M., Callard, L., Chiverrell, R.C., Dove, D., Moreton, S., Roberts, D., Duller, G.A.T., Ó Cofaigh, C., 2019. Ice stream demise dynamically conditioned by trough shape and bed strength (Accepted). Sci. Adv.

Chiverrell, R.C., Smedley, R.K., Small, D., Ballantyne, C., Burke, M., Callard, L., Clark, C.D., Duller, G.A.T., Evans, E., Fabel, D., Landeghem, K.V., Livingstone, S.J., Cofaigh, C., Roberts, D., Saher, M., Scourse, J., Thomas, G.S.P., Wilson, P., 2018. Ice margin oscillations during deglaciation of the northern Irish Sea Basin. J. Quat. Sci. 33, 739–762.

Colarossi, D., Duller, G.A.T., Roberts, H.M., Tooth, S., Lyons, R., 2015. Comparison of paired quartz OSL and feldspar post-IR IRSL dose distributions in poorly bleached fluvial sediments from South Africa. Quat. Geochronol. 30, 233–238.

Duller, G.A.T., 2008. Single grain optical dating of Quaternary sediments: why aliquot size matters in luminescence dating. Boreas 37, 589e612.

Fu, X., Li, S.-H., Li, B., 2015. Optical dating of aeolian and fluvial sediments in north Tian Shan range, China: luminescence characteristics and methodological aspects. Quat. Geochronol. 30, 161–167.

Gaar, D., Lowick, S.E., Preusser, F., 2014. Performance of different luminescence approaches for the dating of known-age glaciofluvial deposits from northern Switzerland. Geochronometria 41, 65–80.

Galbraith, R.F., Laslett, G.M., 1993. Statistical models for mixed fission track ages. Nucl. Tracks Radiat. Meas. 21, 459–470.

Galbraith, R.F., Roberts, R.G., Laslett, G.M., Yoshida, H., Olley, J.M., 1999. Optical dating of single and multiple grains of quartz from Jinmium rock shelter, northern Australia: Part I, experimental design and statistical models. Archaeometry 41, 339–364.

Godfrey-Smith, D.I., Huntley, D.J., Chen, W.-H., 1988. Optical dating studies of quartz and feldspar sediment extracts. Quat. Sci. Rev. 7, 373–380.

Guérin, G., Christophe, C., Philippe, A., Murray, A.S., Thomsen, K.J., Tribolo, C., Urbanova, P., Jain, M., Guibert, P., Mercier, N., Kreutzer, S., Lahaye, C., 2017. Absorbed dose, equivalent dose, measured dose rates, and implications for OSL age estimates: introducing the average dose model. Quat. Geochronol. 41, 163–173.

Huntley, D.J., Lamothe, M., 2001. Ubiquity of anomalous fading in K-feldspars and the measurement and correction for it in optical dating. Can. J. Earth Sci. 38, 1093–1106.

Jerlov, N.G., 1970. Light: general introduction. In: Kinne, O. (Ed.), Marine Ecology. Wiley-Interscience, New York, pp. 95–102.

Kars, R.H., Reimann, T., Ankjærgaard, C., Wallinga, J., 2014a. Bleaching of the post-IR IRSL signal: new insights for feldspar luminescence dating. Boreas 43, 780–791.

Kars, R.H., Reimann, T., Wallinga, J., 2014b. Are feldspar SAR protocols appropriate for post-IR IRSL dating? Quat. Geochronol. 22, 126–136.

King, G.E., Robinson, R.A.J., Finch, A.A., 2014. Towards successful OSL sampling strategies in glacial environments: deciphering the influence of depositional processes on bleaching of modern glacial sediments from Jostedalen, Southern Norway. Quat. Sci. Rev. 89, 94–107.

Kolb, T., Fuchs, M., 2018. Luminescence dating of pre-Eemian (pre-MIS 5e) fluvial terraces in Northern Bavaria (Germany) – benefits and limitations of applying a pIRIR225-approach. Geomorphology 321, 16–32.

Kook, M.H., Lapp, T., Murray, A.S., Thiel, C., 2012. A Risø XRF attachment for major element analysis of aliquots of quartz and feldspar separates. In: UK Luminescence and ESR Meeting, Aberystwyth, September 2012, pp. 37 2012.

Kronborg, C., 1983. Preliminary results of age determination by TL of interglacial and interstadial sediments. PACT 9, 595–606.

Krbetschek, M.R., Götze, J., Dietrich, A., Trautmann, T., 1997. Spectral information from minerals relevant for luminescence dating. Radiat. Meas. 27, 695–748.

McCarroll, D., Stone, J., Ballantyne, C.K., Scourse, J.D., Fifield, L.K., Evans, D.J.A., Hiemstra, J.F., 2010. Exposure-age constraints on the extent, timing and rate of retreat of the last Irish Sea ice stream. Quat. Sci. Rev. 29, 1844–1852.

Möller, P., Murray, A.S., 2015. Drumlinised glaciofluvial and glaciolacustrine sediments on the Småland peneplain, South Sweden – new information on the growth and decay history of the Fennoscandian Ice Sheets during MIS 3. Quat. Sci. Rev. 122, 1–29.

Murray, A.S., Wintle, A.G., 2000. Luminescence dating of quartz using an improved single-aliquot regenerative-dose protocol. Radiat. Meas. 32, 57–73.

Prescott, J.R., Hutton, J.T., 1994. Cosmic ray and gamma ray dosimetry for TL and ESR. Nucl. Tracks Radiat. Meas. 14, 223–227.

Preusser, F., Ramseyer, K., Schlüchter, C., 2006. Characterisation of low OSL intensity quartz from the New Zealand Alps. Radiat. Meas. 41, 871–877.

Qin, J., Chen, J., Li, Y., Zhou, L., 2018. Initial sensitivity change of K-feldspar pIRIR signals due to uncompensated decrease in electron trapping probability: evidence from radiofluorescence measurements. Radiat. Meas. 120, 131–136.

Reimann, T., Thomsen, K.J., Jain, M., Murray, A.S., Frechen, M., 2012. Single-grain dating of young sediment using the pIRIR signal from feldspar. Quat. Geochronol. 11, 28–41.

Roberts, H.M., 2012. Testing Post-IR IRSL protocols for minimising fading in feldspars, using Alaskan loess with independent chronological control. Radiat. Meas. 47 (9), 716–724.

Rowlands, B.M., 1971. Radiocarbon evidence of the age of an Irish Sea glaciation in the Vale of Clwyd. Nature 230, 9–11.

Sanderson, D.C.W., Bishop, P., Stark, M., Alexander, S., Penny, D., 2007. Luminescence dating of canal sediments from Angkor borei, Mekong Delta, Southern Cambodia. Quat. Geochronol. 2, 322–329.

Small, D., Smedley, R.K., Chiverrell, R.C., Scourse, J.D., Ó Cofaigh, C., Duller, G.A.T., McCarroll, D., McCarron, S., Fabel, D., Gheorghiu, D.M., Xu, S., Clark, C., 2018. Trough geometry was a greater influence than climate-ocean forcing in regulating retreat of the marine-based Irish-Sea Ice Stream. Geol. Soc. Am. Bull. https://doi.org/10.1130/B31852.1.

Smedley, R.K., Duller, G.A.T., 2013. Optimising the reproducibility of measurements of the post-IR IRSL signal from single-grains of feldspar for dating. Anc. TL 31 (2), 49–58.

Smedley, R.K., Duller, G.A.T., Pearce, N.J.G., Roberts, H.M., 2012. Determining the K-content of single grains of K-feldspar for luminescence dating. Radiat. Meas. 47, 790–796.

Smedley, R.K., Duller, G.A.T., Roberts, H.M., 2015. Assessing the bleaching potential of the post-IR IRSL signal for individual K-feldspar grains: implications for single-grain dating. Radiat. Meas. 79, 33–42.

Smedley, R.K., Pearce, N.J.G., 2016. Internal U and Th concentrations of K-feldspar grains: implications for luminescence dating. Quat. Geochronol. 35, 16–25.

Smedley, R.K., Glasser, N.F., Duller, G.A.T., 2016. Luminescence dating of glacial advances at Lago buenos Aires (~46 °S), Patagonia. Quat. Sci. Rev. 134, 59–73.

Smedley, R.K., Scourse, J.D., Small, D., Hiemstra, J.F., Duller, G.A.T., Bateman, M.D., Burke, M.J., Chiverrell, R.C., Clark, C.D., Davies, S.M., Fabel, D., Gheorghiu, D.M., McCarroll, D., Medialdea, A., Xu, S., 2017a. New age constraints for the limit of the British-Irish ice Sheet on the isles of Scilly. J. Quat. Sci. 32, 48–62.

Smedley, R.K., Chiverrell, R.C., Burke, M.J., Duller, G.A.T., Thomas, G.S.P., Clarke, C., Scourse, J., 2017b. Internal dynamics condition millennial-scale oscillations of a retreating ice stream margin. Geology 45, 787–790.

Stevens, T., Buylaert, J.-P., Thiel, C., Újvári, G., Yi, S., Murray, A.S., Frechen, M., Lu, H., 2018. Ice-volume-forced erosion of the Chinese Loess Plateau global Quaternary stratotype site. Nat. Commun. 9 (1), 983.

Thiel, C., Buylaert, J.-P., Murray, A., Terhorst, B., Hofer, I., Tsukamoto, S., Frechen, M., 2011. Luminescence dating of the Stratzing loess profile (Austria) – Testing the potential of an elevated temperature post-IR IRSL protocol. Quat. Int. 234, 23–31.

Thomsen, K.J., Murray, A.S., Bøtter-Jensen, L., 2005. Sources of variability in OSL dose measurements using single grains of quartz. Radiat. Meas. 39, 47–61.

Thomsen, K.J., Murray, A.S., Bøtter-Jensen, L., Kinahan, J., 2007. Determination of burial dose in incompletely bleached fluvial samples using single grains of quartz. Radiat. Meas. 42 (3), 370–379.

Thomsen, K.J., Murray, A.S., Jain, M., Bøtter-Jensen, L., 2008. Laboratory fading rates of various luminescence signals from feldspar-rich sediment extracts. Radiat. Meas. 43, 1474–1486.

Trauerstein, M., Lowick, S.E., Preusser, F., Schlunegger, F., 2014. Small aliquot and single grain IRSL and post-IR IRSL dating of fluvial and alluvial sediments from the Pativilca valley, Peru. Quat. Geochronol. 22, 163–174.

Trauerstein, M., Lowick, S., Preusser, F., Veit, H., 2017. Testing the suitability of dim sedimentary quartz from northern Switzerland for OSL burial dose estimation. Geochronometria 44, 66–76.